East European Journal of Physics. **2.** 383-397 (2025)
DOI:10.26565/2312-4334-2025-2-47 ISSN 2312-4334

IMPACT OF JOULE HEATING AND HYDRO-MAGNETIC EFFECTS ON MIXED CONVECTION IN POROUS CAVITY USING LATTICE BOLTZMANN METHOD

C. Venkata Lakshmi[a], Anuradha Aravapalli[a], K. Venkatadri[b]*, O. Anwar Bég[c], V. Ramachandra Prasad[d]

[a]*Department of Applied Mathematics, Sri Padmavati Mahila Visvavidyalayam, Tirupati, Andhra Pradesh - 517502, India*
[b]*Department of Mathematics, Mohan Babu University (Erstwhile Sree Vidyanikethan Eng. Coll.), Tirupati Andhra Pradesh-517 102, India*
[c]*Multi-Physical Engineering Sciences Group, Aeronautical/Mechanical Engineering, Salford University, Corrosion Lab, 3-08, SEE Building, Manchester, M54WT, UK*
[d]*Department of Mathematics, School of Advanced Sciences, Vellore Institute of Technology, Vellore, Tamil Nadu 632014, India*
**Corresponding Author e-mail: venkatadri.venki@gmail.com*
Received March 1, 2025; revised May 11, 2025; accepted May 15, 2025

In the current paper, a comprehensive examination is carried out to investigate heat transmission under the influence of several factors that include magnetic field, moving lid, porous medium, and joule heating within a lid-driven cavity (LDC). The cavity features a moving lid, vertical walls with thermally insulated boundaries, and horizontal walls kept at uniform temperatures T_h (bottom) and T_c (top). The objective of the study is to analyze mixed convective heat transfer behavior of the system using contour plots to visualize the flow and thermal pattern under the various considered parameters: Richardson numbers ($0.01 \leq Ri \leq 10$), and Joule heating parameters ($0 \leq J \leq 10^{-5}$), Hartmann numbers ($0 \leq Ha \leq 30$), and Darcy numbers ($0.001 \leq Da \leq 0.1$). The lattice Boltzmann method (LBM) is applied to employ the governing transport equations. The Joule heating effects are critical in systems where internal heat generation must be controlled, such as in electrical systems or battery cooling, where resistive heating may either aid or hinder the desired thermal dynamics.
Keywords: *Lattice Boltzmann method (LBM); Lid-driven Cavity; Magnetohydrodynamics; Mixed convection; Joule heating; Porous medium*
PACS: 44.05.+e, 47.11.-j, 41.20.−q, 47.15.Rq, 47.65.-d, 47.55.pb, 44.30.+v

1. INTRODUCTION

Convective heat transfer has been the focus of extensive research by scientists and engineers seeking fluids with enhanced thermophysical properties. Recent studies have concentrated on innovative techniques to improve heat transfer systems, with the development of nanofluids emerging as a pivotal strategy. Nanofluids are fluids that contain suspended nanoparticles smaller than 100 nanometres, which contribute to several advantageous characteristics, such as increased thermal conductivity and stability, as well as improved heat transfer capabilities compared to traditional fluids. Addressing the issue of overheating during operation is crucial, as it can significantly shorten the lifespan of modern electronic devices and, in extreme cases, lead to system failures. Therefore, implementing effective heat transfer solutions to efficiently dissipate excess heat from these devices is vital. Nanofluids show great promise as coolants and Fluids used for heat transfer in various electronic applications, featuring computer chips, LED lights, and solar cells, ultimately enhancing their performance and reliability.

One of the significant areas of study has been the influence of magnetic fields on mixed convection in enclosures. Turabi and Munir [1] conducted CFD simulations to inspect the effects of magnetohydrodynamics (MHD) on combined convection of thermal flow in a LDC equipped with cylinder using Casson fluid. As a result of their study the application of a field of magnetism suppresses convective currents due to the Lorentz forces reduce the rate of motion due to their generation in heat transfer efficiency. Similarly, as a result of Oztop and Dagtekin's [2] study, mixed convection occurred in an enclosure driven by both sides of the cavity under differential heating and found that Richardson and Hartmann numbers play crucial roles in controlling the fluid flow structure and thermal distribution. In a more advanced study, the study was reported by Parveen et al. [3] investigated magnetohydrodynamic (MHD) mixed thermal flow within an oblique wavy enclosure packed with ferrofluid under lid-driven conditions, incorporating heat generation and absorption effects. Their findings indicated that wavy geometries enhance thermal mixing, but stronger magnetic fields dampen convective currents, leading to a decline in heat transfer. Further insights into the impact of strong magnetic fields were provided by Zikanov et al. [4], who examined mixed convection in duct and pipe flows, highlighting turbulence suppression and reduced convective heat transfer under intense MHD conditions.

The effect of nanofluids in mixed convection systems has also been extensively studied to leverage their superior thermal conductivity properties. Devi et al. [5] conducted an insightful exploration of thermal flow behavior within an enclosure. Their study examines the influence of applied magnetic field and the presence of a heated square blockage, contributing valuable knowledge to the field. Their numerical simulations revealed that the buoyancy ratio and nanoparticle volume fraction significantly affect the heat and mass transfer characteristics. Mondal et al. [6] explored

Cite as: C.V. Lakshmi, A. Aravapalli, K. Venkatadri, O.A. Bég, V.R. Prasad, East Eur. J. Phys. 2, 383 (2025), https://doi.org/10.26565/2312-4334-2025-2-47

similar phenomena in a trapezoidal enclosure and emphasized the role of heat generation and absorption in modulating temperature gradients. In another study, Parveen and Mahapatra [7] examined entropy generation in a nanofluid-filled curved chamber, demonstrating that increasing the magnetic field strength suppresses convective currents, resulting in higher thermal irreversibility. Yu et al. [8] extended this research by incorporating Buongiorno's nanofluid model to analyze the effects of Brownian motion and thermophoresis on heat transfer in an inclined lid-driven cavity, concluding that these mechanisms enhance thermal conductivity but alter velocity profiles in complex ways. Mahmood and Khan [9] further contributed by assessing the Darcy-Forchheimer effect in mixed convection of nanofluids, showing that nanoparticle aggregation leads to significant changes in flow stability and heat transfer performance.

Geometrical modifications and internal obstructions in LDC's have been another focus area. Munshi et al. [10] analyzed mixed convection within square cavity containing elliptic heated blocks with corner heaters, observing that heat sources at the corners create asymmetric flow patterns that influence convective heat transport. Similarly, Sivasankaran et al. [11] studied forced convection in an oblique LDC with partially heated elements, reporting that inclination angles significantly impact fluid circulation and overall heat dissipation rates. Khanafer and Chamkha [12] inspected combined convection in a porous LDC, concluding that permeability parameters, such as the Darcy number, govern the dominance of either conduction or convection-driven heat transfer. Additionally, Munshi et al. [13] focused on Mixed convection within a square enclosure containing a porous medium and featuring pairs of heat sources and sinks, demonstrating that the arrangement of heat sources strongly affects temperature distribution and vortex formation within the cavity.

Several recent studies have focused on advancing numerical methodologies to Make the computations more accurate and efficient of mixed convection simulations. Nawaz et al. [14] explore an analysis of Williamson non-Newtonian nanofluid flow over oscillatory sheets using a two-stage multi-step numerical technique, achieving improved convergence and stability. Qaiser et al. [15] performed a numerical assessment of Walters-B nanofluid over a elongating sheet incorporating Newtonian heating and mass transfer, utilizing finite difference methods to obtain precise predictions of temperature and velocity fields. These advancements in numerical techniques play a crucial role in solving complex mixed convection problems, particularly in configurations involving nanofluids, MHD, and non-Newtonian fluids. The transient behavior of MHD convection has been significantly enhanced through the contributions of various researchers. Sheremet et al. [16] utilized finite element techniques to analyze time-dependent flows, highlighting the crucial role of computational precision in accurately capturing dynamic phenomena, particularly in the context of geothermal viscosity. Building on this, Alam et al. [17] effectively applied the Finite Element Method to investigate MHD natural convection, demonstrating the method's capability in managing complex geometries and heat sources on base walls. Geridonmez et al. [18] made valuable contributions by examining mixed thermal flow in a driven cavity influenced by a partial magnetic field, thus enriching the understanding of cavity flows in the presence of combined convection fields. Furthermore, Suchana et al. [19] explored the effects of Lorentz force and non-uniform thermal conditions on convection in trapezoidal enclosures, employing FEM to shed light on these interactions. Mohan et al. [20] analyzed double-diffusive convection in porous cavities under MHD effects using an FVM approach, further expanding the field's knowledge base. Additionally, Bakar et al. [21] and Moria [22] have investigated specific configurations, such as inclined magnetic fields and heat-generating blocks respectively, which contributed to a deeper understanding of unique cavity designs. Meanwhile, researchers like Wang et al. [23] and Nee [24] have adopted spectral methods and hybrid FDM-LBM techniques to improve computational accuracy in modeling MHD convection, demonstrating a collaborative effort to advance the field comprehensively.

The extensive research into MHD convection in porous cavities provides valuable insights into the complex interactions among magnetic fields, the properties of porous media, and boundary conditions that influence heat transfer. The application of advanced numerical techniques such as FEM, LBM, FVM, and hybrid approaches has significantly improved the accuracy and relevance of these studies. This progress offers a deeper understanding of transient, steady-state, and double-diffusive behaviours in various configurations. Nonetheless, there are promising opportunities for further exploration. In particular, more comprehensive studies that integrate Joule heating effects, hydro-magnetic mixed convection, and porous medium interactions under realistic boundary and operational conditions are needed. Investigating the effects of internal heat generation due to Joule heating, alongside the complex dynamics of buoyancy-driven convection, forced convection, and magnetic fields, presents a crucial area for future research. Moreover, while the Lattice Boltzmann Method has demonstrated its effectiveness across numerous studies, its application in simulating multi-physics scenarios remains underexplored. To bridge these gaps, the current study intends to utilize Thermal Lattice Boltzmann simulations to examine hydro-magnetic mixed convective transport phenomena in a square cavity filled with a porous medium and subjected to an inclined magnetic field. The configuration involves air-filled cavities that are with heat applied to the lower side and cooling on the upper side, with Joule heating effects incorporated. This research aims to enhance our understanding of the intricate interactions between magnetic and thermal forces, ultimately contributing to the optimization of thermal management systems.

Research Gaps and Motivation for The Current Study

Despite extensive research on MHD mixed convection in porous enclosures, several critical gaps remain in understanding the complex interactions between magnetic fields, porous media, lid-driven forces, and Joule heating effects:

- The combined effects of Joule heating, inclined magnetic fields, and lid-driven forces in a porous enclosure have not been fully explored.
- Existing studies (e.g., [4, 7, 15]) have investigated entropy generation and thermal transport in nanofluid-based MHD systems but overlooked Joule heating effects.
- Existing studies on nanofluid convection focus primarily on Brownian motion and thermophoresis, with limited investigations into electromagnetic heating effects.
- While some studies (e.g., [14]) have explored LBM for nanofluid convection, its application to MHD mixed convection with Joule heating and porous media interactions remains limited.
- While LBM has demonstrated effectiveness in modelling MHD flows, its potential for simulating Joule heating-driven mixed convection remains underutilized.

To address these gaps, the present study focuses on Thermal Lattice Boltzmann simulation of hydro-magnetic mixed convective transport phenomena in a square cavity filled with a porous medium, subjected to an inclined magnetic field. The bottom-heated and top-cooled configuration is chosen to mimic practical thermal management scenarios, while Joule heating effects are incorporated to analyze their impact on heat and fluid transport.

3. MATHEMATICAL FORMULATION

The computational model of the lid-driven square cavity, as illustrated in **Figure 1**, presents an intriguing study of fluid dynamics. This cavity, characterized by equal height and width (H), features a top boundary sustained at a fixed temperature (T_c) while moving to the right at a steady velocity (U_0). The bottom boundary is kept at a constant elevated temperature (T_h), while the vertical side boundaries are thermally insulated to maintain heat distribution within the system. To enhance the practicality of numerical simulations, several assumptions have been implemented. The fluid flow within the cavity is analyzed as a two-dimensional, laminar, and incompressible flow. Additionally, an inclined field of magnetism (B_0) is imposed across the cavity, complemented by a downward gravitational force (g). This model innovatively utilizes a lid-driven cavity with permeable characteristics, treating it as an isotropic and homogeneous porous medium. This medium is defined by constant permeability and porosity, allowing for uniform fluid passage through it. The thermal gradients present across the cavity walls result in density differentials that, along with the lid motion, facilitate the fluid movement within the cavity. The operational effectiveness of the permeable zone is governed by the principle of local thermal equilibrium, a critical condition for its functionality. Furthermore, under the Boussinesq approximation, the analysis intentionally excludes factors such as radiation, viscous dissipation and internal heat generation as a joule heating.

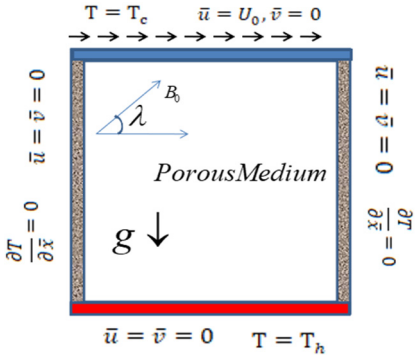

Figure 1. Physical model of the geometry

3. LATTICE BOLTZMANN METHOD

The Lattice Boltzmann Method (LBM) offers a highly versatile and efficient framework for simulating fluid dynamics and related phenomena. Its mesoscopic approach, coupled with computational efficiency and adaptability, positions it as a preferred option for a wide range of scientific and engineering applications. Among the various collision operators available in LBM, the BGK (Bhatnagar-Gross-Krook) model is particularly noteworthy for its simplicity and extensive use in the field. When applied to a D2Q9 lattice—a two-dimensional grid comprising nine discrete velocity directions—the BGK model serves as a solid foundation for fluid dynamics simulations in two dimensions. This method effectively balances computational efficiency with accuracy, making it a valuable tool for researchers and engineers engaged in two-dimensional fluid dynamics studies. The flow field and distribution function of the SRT (single relaxation time) model within the BGK LBM, especially when incorporating external forces, can be articulated as follows [25-27]: f and g, refers for the flow and temperature fields of distribution functions, respectively

$$f_i\left(x+c_i\Delta t,t+\Delta t\right)=f_i\left(x,t\right)-\frac{1}{\tau_f}\left(f_i\left(x,t\right)-f_i^{eq}\left(x,t\right)\right)+\Delta tF_i, \tag{1}$$

$$g_i\left(x+c_i\Delta t,t+\Delta t\right)=g_i\left(x,t\right)-\frac{1}{\tau_g}\left(g_i\left(x,t\right)-g_i^{eq}\left(x,t\right)\right)+S_i, \tag{2}$$

the local equilibrium particle distribution function for flow and temperature are calculated from Eqs. (3) and (4).

$$f_i^{eq} = w_i \rho \left[1 + \frac{3}{c^2}(c_i \bullet u) + \frac{9}{2c^4}(c_i \bullet u)^2 - \frac{3}{2c^2}(u \bullet u) \right], \tag{3}$$

$$g_i^{eq} = w_i T \left[1 + \frac{1}{c^2}(c_i \bullet u) \right]. \tag{4}$$

The D2Q9 model is utilized in this study for analyzing flow and temperature; The lattice weights are calculated as follows;

$$w_i = \begin{cases} \frac{4}{9}, i = 0 \\ \frac{1}{9}, i = 1,2,3,4 \\ \frac{1}{36}, i = 5,6,7,8 \end{cases} \tag{5}$$

The discrete velocities are obtained from the eq. (6).

$$c_{\mathbf{i}} = \begin{cases} 0 & i = 0 \\ \left(\cos\left[\frac{(i-1)\pi}{4} \right], \sin\left[\frac{(i-1)\pi}{4} \right] \right) & i = 1,2,3,4 \\ \sqrt{2}\left(\cos\left[\frac{(i-1)\pi}{4} \right], \sin\left[\frac{(i-1)\pi}{4} \right] \right) & i = 5,6,7,8 \end{cases} \tag{6}$$

Here $c = \frac{\Delta x}{\Delta t}$ is the lattice speed.

macroscopic pressure is determined for incompressible fluid flow by

$$P = \rho c_s^2, (c_s^2 = \frac{c^2}{3}) \tag{7}$$

The single relaxation times are given by

$$\upsilon = \left[\tau_f - \frac{1}{2} \right] {c_s}^2 \Delta t \text{ and } \alpha = \left[\tau_g - \frac{1}{2} \right] {c_s}^2 \Delta t \tag{8}$$

The external body force with LBM as

$$F_i = w_i . F . \frac{c_i}{c_s^2} \tag{9}$$

The value $c_s^2 = \frac{c^2}{3}$, Joule heating acts as an external source term:

$$S_i = w_i \sigma B_0^2 v^2 \ , \ F_i = w_i . F \tag{10}$$

$$F = Fx + Fy$$

$$Fx = -w_k 9 \rho \frac{\upsilon}{K} u + 3 w_k \rho A \left(v \sin\lambda \cos\lambda - u \sin^2\lambda \right), \tag{11}$$

$$Fy = -w_k 9 \rho \frac{\upsilon}{K} v + 3 w_k \rho \left(g\beta \left(T - T_c \right) + A \left(u \sin\lambda \cos\lambda - v \cos^2\lambda \right) \right)$$

Here $A = Ha^2 \frac{\nu}{M^2}$ and $K = DaM^2$

Finally, Macroscopic variables are expressed as:

$$\rho = \sum_i f_i \tag{12}$$

$$\rho u = \sum_i f_i \mathbf{c_i} \tag{13}$$

$$T = \sum_i g_i \tag{14}$$

3.1 Method of mixed convection

The Mach number is considered as 0.1for this simulation. Since, the Mach number for the incompressible flow is Ma < 0.3.

By taking the Mach number, Prandtl number, thermal Grashof number and the thermal diffusivity are employed from definition of:

$$\upsilon = \frac{1}{\sqrt{Gr}} MaMc\,. \tag{15}$$

The speed of the lattice is constant and it considered as $c = \frac{1}{\sqrt{3}}$.

The condition for the lid-driven speed is utilized the following:

$$U_0 = \frac{\mathrm{Re}\,\upsilon}{M}\,. \tag{16}$$

Table 1. The analysis of Grid independence for ψ_{min} and Nu_a at $Pr = 0.71, Re = 100$, $Ri = 1$, and $Ha = 0, J = 0$.

Grid size	$\lvert\psi_{\min}\rvert$	% Error	Nu_a	% Error
41×41	0.5992	----	3.1214	----
41×41	0.8430	0.4124	3.0030	0.03793
81×81	1.0580	0.2551	2.9342	0.02291
101×101	1.2491	0.1806	2.8910	0.01472
121×121	1.4196	0.1365	2.8636	0.00948

Table 2. Average Nusselt Number Comparison for a Mixed convection in a Lid-Driven Cavity at Gr = 100 and Pr = 0.71.

Re	Ri	Tiwari and Das [28]	Iwatsu et al. [29]	Present
100	0.01	2.10	1.94	2.09
400	0.00062	3.85	3.84	4.0808
1000	0.0001	6.33	6.33	6.5469

3.2. Boundary Conditions

Solid (or no slip) walls are considered bounce-back boundary conditions. At the top boundary, the particle distributions are considered as follows:

$$\begin{aligned}
\rho_N &= \frac{1}{1+v_N}\left(f_0 + f_2 + f_3 + 2\left(f_2 + f_6 + f_5\right)\right)\\
f_4 &= f_2 - \frac{2}{3}\rho_N v_N\\
f_7 &= f_5 + \frac{1}{2}\left(f_1 - f_3\right) - \frac{1}{6}\rho_N v_N - \frac{1}{2}\rho_N u_N\\
f_8 &= f_6 + \frac{1}{2}\left(f_1 - f_3\right) - \frac{1}{6}\rho_N v_N + \frac{1}{2}\rho_N u_N
\end{aligned} \tag{17}$$

u and v refer horizontal and vertical velocity on the north (top) boundary, respectively.

The adiabatic wall (East and West), bounce back boundary conditions are used. Temperature at bottom and top walls are known in the bottom wall, $T = T_h$. Since we are using D2Q9, the unknowns are computed as follows.

$$\begin{aligned}
g_2 &= \left(T_h - T_c\right)\left(w_2 + w_4\right) - g_4\\
g_5 &= \left(T_h - T_c\right)\left(w_5 + w_7\right) - g_7\\
g_6 &= \left(T_h - T_c\right)\left(w_6 + w_8\right) - g_8
\end{aligned} \tag{18}$$

In terms of the local Nusselt number and the average value on hot wall, they can be calculated as follows:

$$Nu = \frac{L}{\Delta T}\frac{\partial T}{\partial y} \tag{19}$$

$$Nu_a = \frac{1}{L}\int_0^L Nu\,dx \tag{20}$$

Finally, the stream function can be defined in a manner consistent with its standard definition, as outlined below:

$$u = \frac{\partial \psi}{\partial y}, v = -\frac{\partial \psi}{\partial x} \tag{21}$$

The value of the stream function (ψ) on all boundary walls is considered as zero.

3.3. Grid Independence and Validation of LBM

Table 2 presents the results of the grid independence test conducted across various grid sizes: 41×41, 61×61, 81×81, 101×101, and 121×121. The computational grids were systematically refined and optimized to achieve an accurate discretization of the governing equations within the examination domain. Upon analysis, no significant differences were observed between the grid sizes, particularly between the 101×101 and 121×121 configurations. As a result, the 101×101 grid size was chosen for the simulations. This decision aligns with the findings of Moallemi and Jang [30], underscoring the importance of conducting a grid independence test to ensure numerical stability and solution accuracy. By minimizing discretization errors, we can effectively capture critical flow and thermal characteristics in our simulations.

The Thermal LBM used in this study has been effectively validated through simulations of lid-driven mixed convection heat transfer at a Reynolds number Re=1000, Pr = 0.1, and Ri = 0.01. As illustrated in Figure 2, the streamline and isotherm patterns derived from the LBM simulation reveal a high degree of alignment with the findings of Moallemi and Jang [30]. This strong correlation highlights the accuracy of the flow structures and thermal distributions captured within LDC. Such validation not only supports the reliability of the numerical method used but also sets a solid foundation for further investigations into hydro-magnetic mixed convection in porous cavities, particularly under varying thermal conditions and influences including inclined magnetic fields and Joule heating.

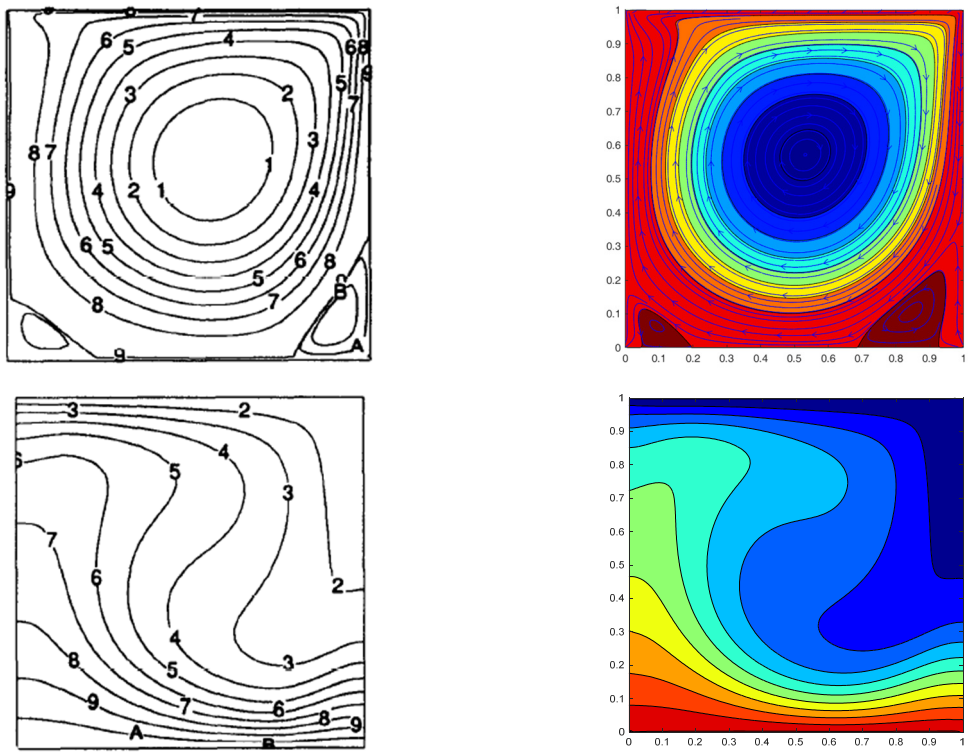

Moallemi et al. [30] Present (LBM)

Figure 2. Comparison results of flow patterns and thermal contours of present and Moallemi et al. [30]

4. RESULTS AND DISCUSSION

This section introduces the graphic diagrams of the simulations concerning the heat and fluid flows of mixed convective flowing in a LDC saturated with porous medium in presence of inclined field of magnetism and joule heating. The density gradients inside the enclosure cause buoyancy forces, leading to the production of streamlines, heatlines, and isotherms. The study investigates the influence of various ranges of involved factors such as Richardson numbers ($0.1 \leq Ri \leq 10$), inclination angle ($0 \leq \lambda \leq 180^0$), Darcy number ($0.001 \leq Da \leq 0.1$), Hartmann number ($0 \leq Ha \leq 30$) and Joule heating parameters ($0 \leq J \leq 10^{-5}$). The $Pr = 0.71$ and $Re = 100$, are kept constant.

Figure 3 presents the influence of the ***Ri*** on the flow and thermal structures within the square cavity. As Ri varies from 0.01 to 10, a clear transition from forced convection to natural convection is observed. At lower Ri values (0.01 and 0.1), inertial forces dominate over buoyancy effects, resulting in strong recirculatory motions and skewed streamlines. The corresponding isotherms exhibit substantial distortion, indicating vigorous convective heat transfer. As Ri increases to 1.0, buoyancy and inertia attain comparative magnitudes, generating more symmetric vortex structures with moderated

thermal gradients. At the highest Ri value considered (Ri = 10), buoyancy forces clearly prevail, leading to weakened circulatory motion and vertically stratified isotherms. The thermal field under these conditions is predominantly governed by conduction, with minimal convective mixing, illustrating the classical characteristics of natural convection dominance.

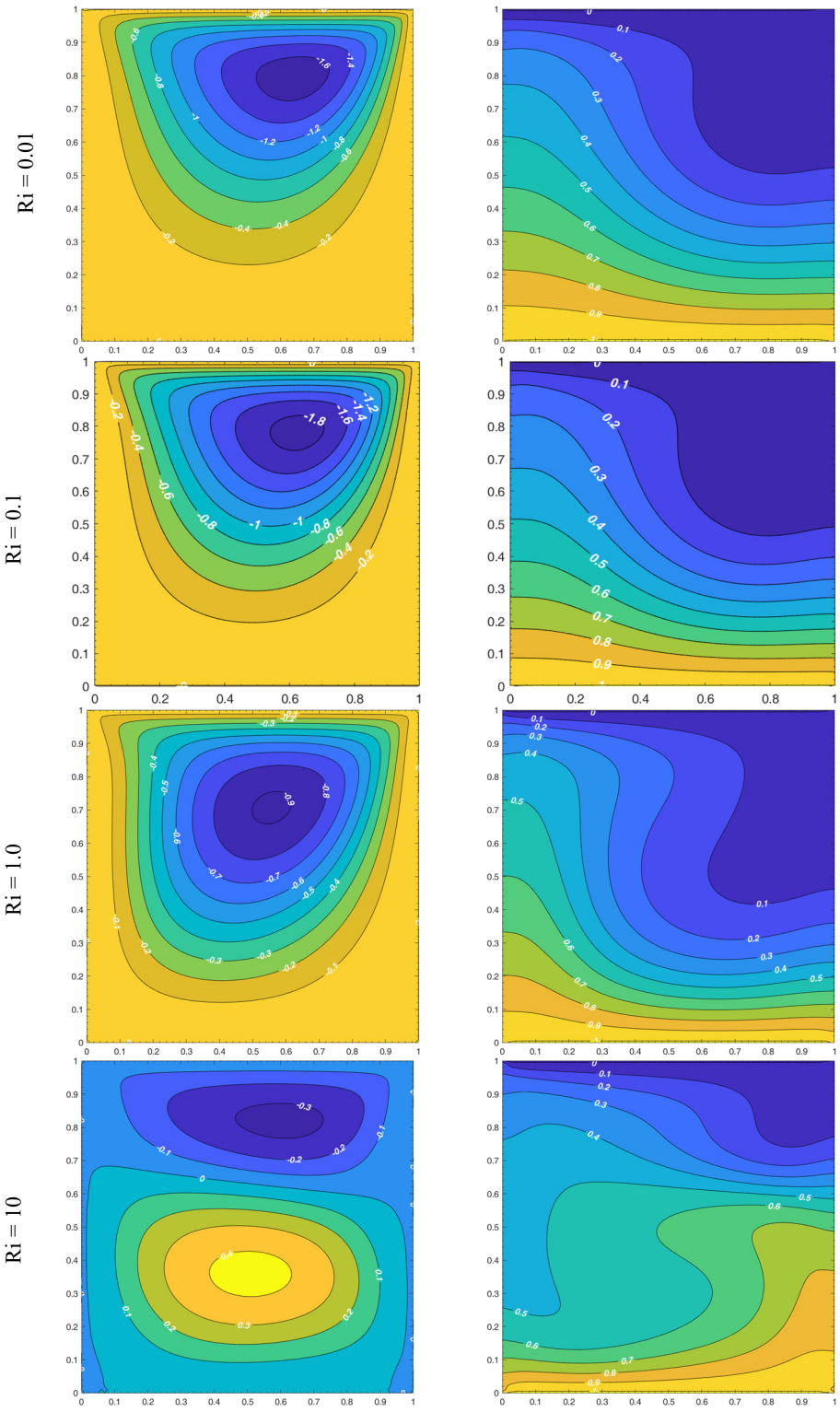

Figure 3. The behavior of streamlines and temperature distribution contour plots for diverse Ri values with fixed Re = 100, $J = 1 \times 10^{-5}$, Ha = 2, Da = 0.1, $\lambda = \pi/4$.

Figure 4 demonstrates the suppressive effect of a magnetic field on the convective flow, illustrated through increasing Hartmann numbers (Ha = 0, 10, 20, 30). In the case Ha = 0, the flow exhibits strong circulation cells, and isotherms show significant distortion due to the active convective transport of heat. Higher Ha values amplify the Lorentz force due to magnetic field-fluid interactions, exerting a decelerating effect. This is evident at Ha = 10 and more

prominently at Ha = 20, where the streamlines become compressed and vortex strength diminishes. At Ha = 30, convective motion is substantially suppressed, and the isotherms tend to align horizontally, marking a shift towards conduction-dominated heat transfer. These results clearly highlight the magnetic field's ability to regulate convective strength and control thermal gradients within the cavity.

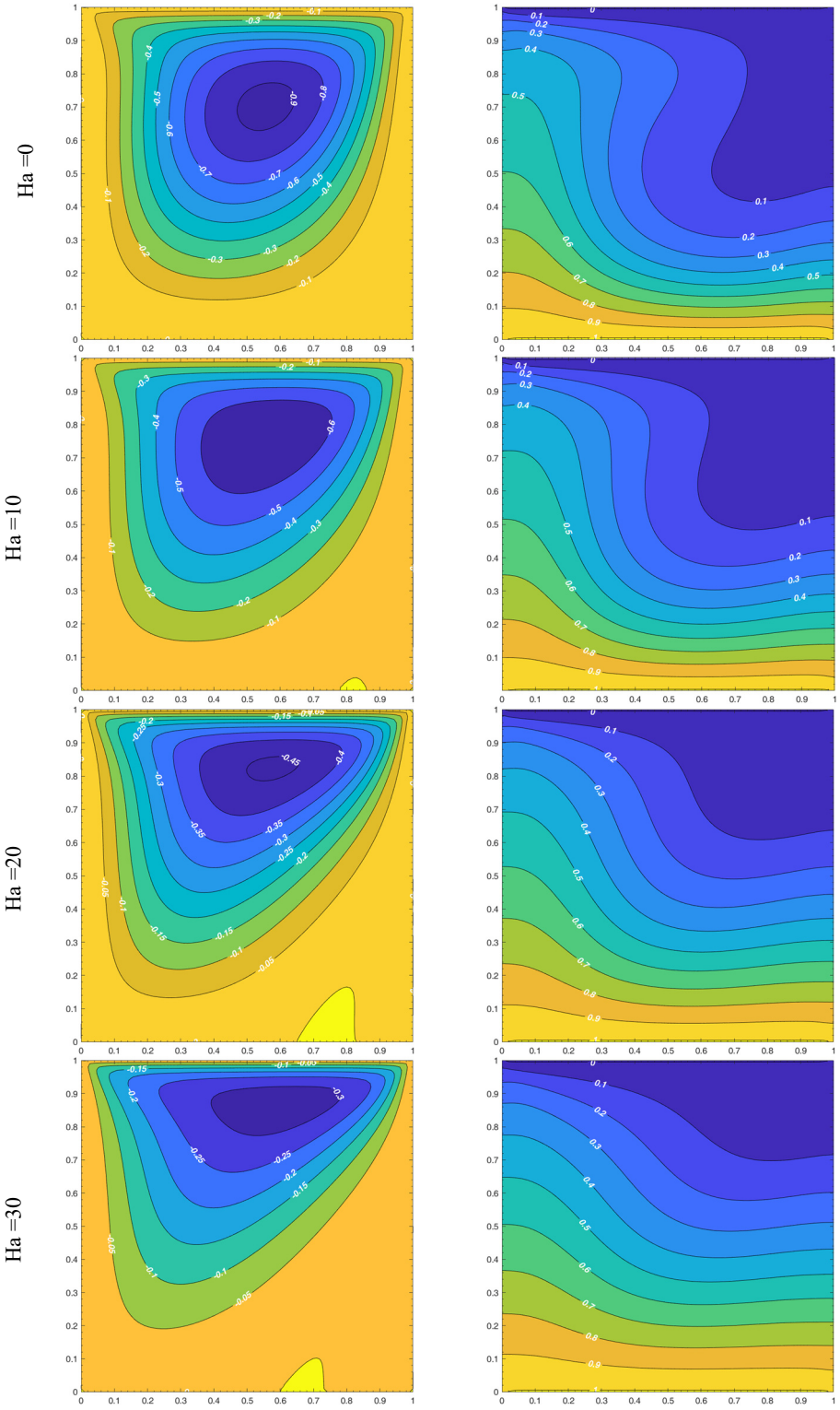

Figure 4. The behavior of streamlines and temperature distribution contour plots for diverse Ha values with fixed Ri = 1, Re = 100, $J = 1 \times 10^{-5}$, Da = 0.1, $\lambda = \pi/4$.

Figure 5 explores the effect of varying the permeability parameter (Da) to assess how the porous medium's permeability influences the transport characteristics. For an effectively non-porous cavity (Da = ∞), the fluid moves freely, yielding strong convection currents and highly perturbed isotherms. As Da is decreased to 0.1 and 0.01, the permeability

of the porous matrix diminishes, increasing the flow resistance. This attenuation in fluid motion results in weaker vortices and a noticeable reduction in isothermal curvature, signifying a gradual suppression of convective heat transport. When Da reaches 0.001, the medium becomes nearly impermeable, and the streamlines collapse into stagnant zones. The isotherms exhibit vertical alignment, characteristic of purely conductive regimes. The observed transition underscores the critical role of porous media in modulating convective intensity and controlling heat flow pathways.

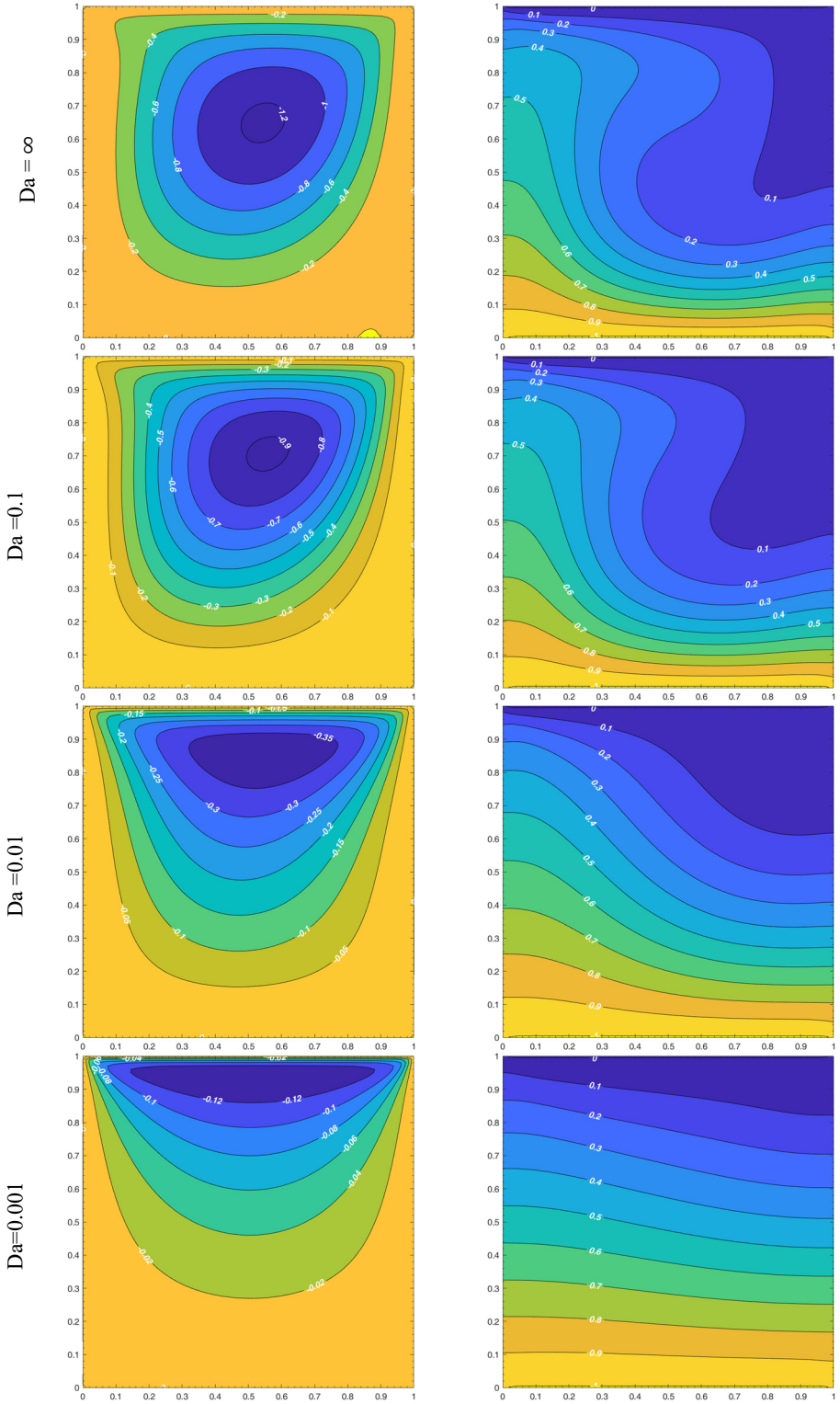

Figure 5. The behavior of streamlines and temperature distribution contour plots for diverse Da values with fixed Ri = 1, Re = 100, $J = 1 \times 10^{-5}$, Ha = 2.0, $\lambda = \pi/4$.

Figure 6 focuses on the impact of the Joule heating parameter (J) on the flow dynamics and temperature distribution. At J = 0, the cavity is unaffected by internal heat generation, and the flow field is governed by buoyancy and inertial

forces alone. The resulting streamline pattern exhibits moderate vortices, and the isotherms reflect smooth, convective bending. As J increases to 0.01 and 0.03, resistive (ohmic) heating due to electromagnetic effects becomes significant. The added thermal energy intensifies buoyancy-driven forces, leading to enhanced vortex strength and increasingly non-uniform isotherm distributions. At J = 0.05, the convective motion becomes even more vigorous, with pronounced distortion in both flow and temperature fields. This escalation of thermal gradients and circulatory activity demonstrates how Joule heating amplifies heat transfer mechanisms by injecting energy directly into the fluid domain, thereby intensifying the hydrothermal interaction under electromagnetic influence.

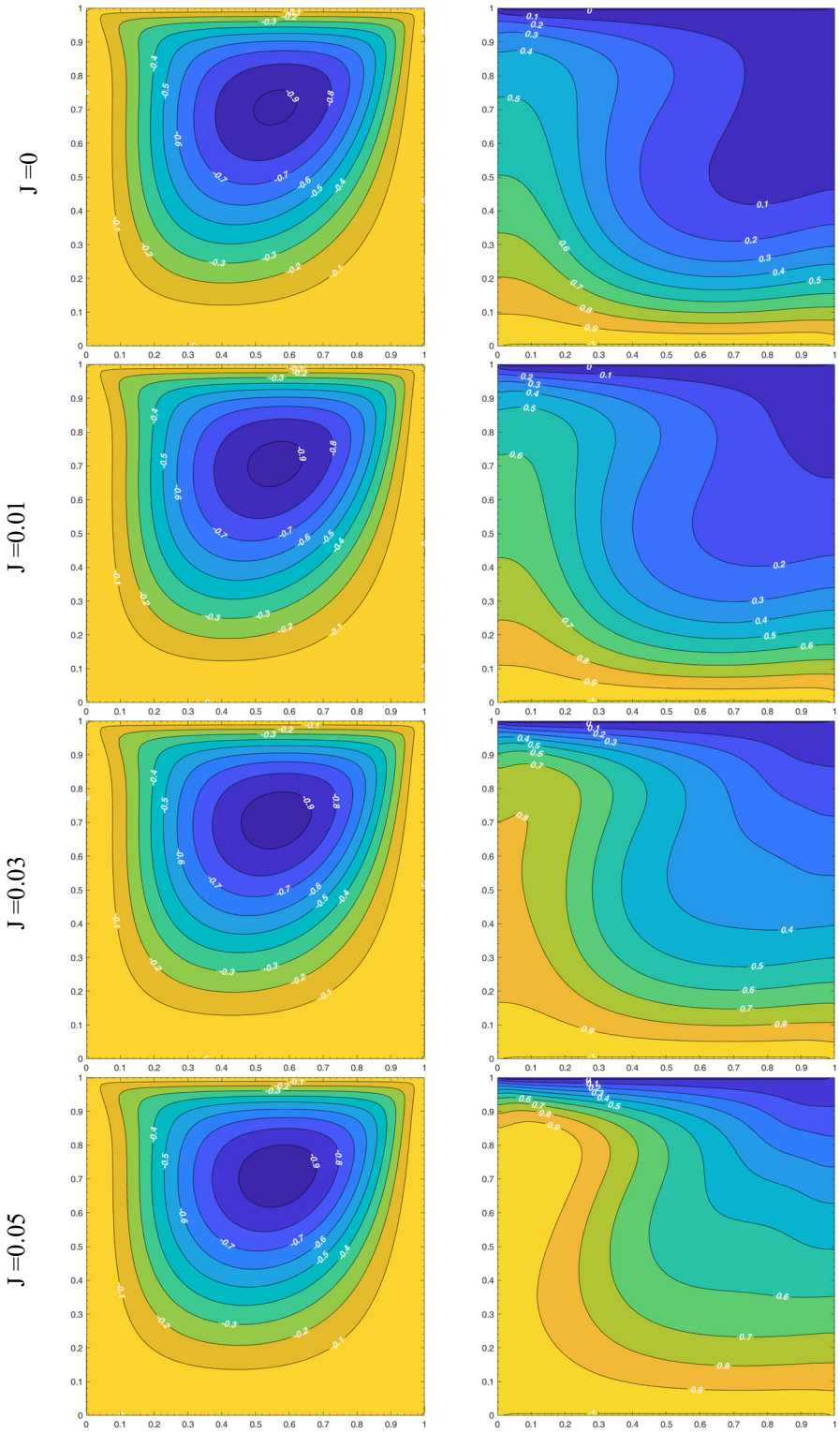

Figure 6. The behavior of streamlines and temperature distribution contour plots for diverse J values with fixed Re = 100, Da = 0.1, Ha = 2, Ri = 1.0, $\lambda = \pi/4$.

Figure 7 depicts how the average Nusselt number (Nu_a) varies with the Hartmann number (Ha) across three distinct Richardson numbers (Ri = 0.1, 1.0, and 10.0). This figure encapsulates the combined effect of magnetic field intensity and buoyancy-to-inertia ratio on thermal transport in the cavity. For all Ri values, it is evident that Nu_a decreases monotonically with increasing Ha, which indicates a progressive suppression of convective heat transfer by the magnetic field. At Ri = 10.0, where buoyancy dominates, Nu_a starts at a significantly higher value (~4.5) and drops steeply as Ha increases, demonstrating that the magnetic damping effect is especially potent when natural convection is dominant. This steep reduction in Nu_a can be attributed to the Lorentz force, which opposes the fluid motion and suppresses thermal plumes that enhance heat transfer in buoyancy-driven flows. For intermediate buoyancy influence (Ri = 1.0), Nu_a also declines with Ha, but the gradient is less severe, reflecting a balance between inertial and buoyancy effects, and a moderated sensitivity to magnetic suppression. At low Ri (0.1), the system is primarily governed by forced convection, and the Nu_a values remain relatively low across all Ha. The impact of increasing Ha under such conditions is more subdued, as the flow is already mechanically driven and less susceptible to Lorentz-induced resistance. The convergence of Nu_a values across different Ri levels at high Ha (>25) suggests that, under strong magnetic fields, conduction becomes the dominant mode of heat transfer, regardless of the initial convective regime.

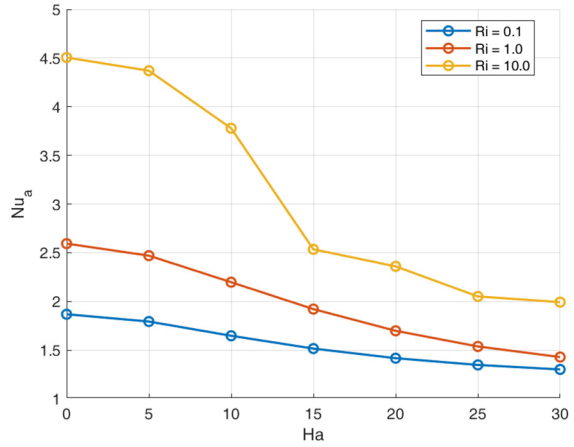

Figure 7. Average Nusselt number (Nu_a) variation with Hartmann number (Ha) with distinct Richardson numbers (Ri).

Figure 8 illustrates the variation Nu_a with respect to the Joule heating parameter (J) for three distinct Ri (Ri = 0.1, 1.0, and 10.0). The results clearly demonstrate a significant decline in Nu_a as J increases, indicating the pronounced influence of resistive (Joule) heating on thermal transport within the cavity. Joule heating acts as an internal volumetric heat source, which leads to temperature homogenization and subsequently diminishes the temperature gradients that drive convective heat transfer.

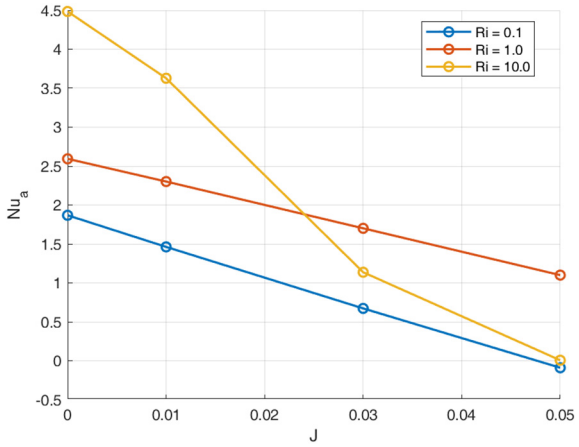

Figure 8. Average Nusselt number (Nu_a) variation with Joule heating parameter (J) with various Richardson numbers (Ri)

For Ri = 10.0, where buoyancy-driven natural convection dominates, the initial Nu_a is notably high (~4.5). However, a sharp decline is observed as J increases, with Nu_a approaching zero at J = 0.05. This underscores the suppressive effect of Joule heating on buoyancy-induced circulation, where thermal diffusion overtakes convective mechanisms. In the case of Ri = 1.0, representing a mixed convection regime, the decrease in Nu_a with increasing J is more gradual, reflecting a competitive balance between forced and natural convection effects being gradually overpowered by Joule heating. For Ri = 0.1, indicative of forced convection dominance, the Nu_a values are the lowest across the board, and exhibit a near-linear decline with J. Notably, at J = 0.05, the Nu_a values for Ri = 0.1 and Ri = 10.0 converge near zero, implying that under

strong internal heating, the nature of convection—whether forced or natural—becomes irrelevant, as conduction becomes the dominant mode of heat transfer. The results collectively reveal that Joule heating can significantly deteriorate convective efficiency, especially in thermally buoyant regimes, due to the suppression of temperature gradients and flow circulation.

Figure 9 presents the variation of the average Nusselt number Nu_a with respect to the inclination angle λ of the applied magnetic field for three different Richardson numbers: Ri=0.1 (forced convection dominant), Ri=1 (mixed convection), and Ri=10 (natural convection dominant). It is observed that for all values of Ri, the average Nusselt number remains nearly constant as λ increases from 0 to π/2. This indicates that the inclination of the non-uniform magnetic field has a minimal impact on the overall heat transfer in the cavity. In particular, the Nu_a values are highest for Ri=10, signifying that natural convection significantly enhances heat transfer independent of the magnetic field's positional alignment. For Ri=0.1, the values of Nu_a are lower, as expected due to the reduced influence of buoyancy, and they too show minimal variation with λ. The negligible slope in each curve suggests that the reorientation of the Lorentz force has little effect on disrupting or altering the thermal boundary layer development and flow structure. This behavior implies that the damping effect imposed by the magnetic field is primarily governed by its magnitude and spatial variation rather than its directional alignment. Therefore, in uniform magnetic strength, altering its inclination angle does not significantly affect convective heat transfer in the cavity under mixed convection conditions.

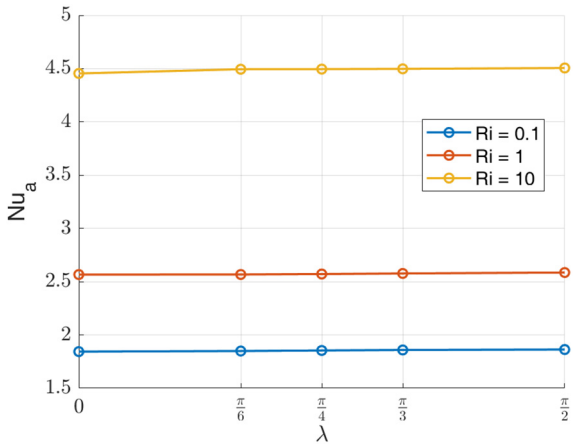

Figure 9. Influence of inclination angle (λ) of magnetic force on average Nusselt number (Nu_a) for different Richardson numbers (Ri)

5. FINAL REMARKS

The study of hydro-magnetic mixed convective transport phenomena in a 2D square cavity, incorporating Joule heating effects and porous media, reveals several critical insights into the underlying physics and parameter interactions. By using the lattice Boltzmann method to simulate fluid dynamics, the study explores the coupling between thermal, flow, and magnetic forces under various dimensionless parameters such as Reynolds number (Re), Hartmann number (Ha), Darcy number (Da), Richardson number (Ri), and the Joule heating parameter (J). The key conclusions are summarized as follows:

- Increasing Ha significantly suppresses fluid motion due to enhanced Lorentz force, which dampens convection and shifts the heat transfer mechanism towards conduction. A higher Ha consistently leads to a lower average Nusselt number.
- As the Hartmann number (Ha) increases from 2 to 30, a significant reduction in fluid circulation is observed. For instance, at **Ha = 30,** streamlines become nearly parallel, indicating **a 70–80%** suppression in convective motion compared to **Ha = 0**, leading to more uniform isotherms and reduced thermal transport.
- At low Ri (e.g., 0.01), forced convection dominates, allowing stronger thermal mixing. As Ri increases, buoyancy becomes more influential, but it is also more susceptible to suppression by magnetic fields and Joule heating.
- An increase in J introduces greater internal heat generation, which intensifies local thermal gradients. However, this effect also increases entropy generation, thereby reducing the overall heat transfer efficiency, especially in buoyancy-driven flows.
- With increasing Joule heating parameter J from 0 to 0.05, internal energy generation enhances local temperature gradients. The peak Nusselt number increases by up to 25%, but spatial uniformity of heat transfer degrades, indicating thermal instability and less efficient global heat transport.
- High Da enables strong convection, producing pronounced vortices and thermal mixing, while, Lower Da reduces permeability, constraining fluid motion. At very low Da, conduction dominates, as indicated by vertical isotherms and diminished flow patterns.
- Changes in the inclination angle of the non-uniform magnetic field (λ) have a relatively minor influence on the overall heat transfer rate, suggesting that the direction of the magnetic field is less critical than its magnitude.

- The highest average Nusselt number is recorded under low Ha (2), low J (0), high Ri (10), and high Da (∞) conditions—signifying strong convective transport. Conversely, Ha = 30, J = 0.05, and Da = 0.001 result in a conduction-dominant regime with significantly reduced heat transfer efficiency.

Limitation.

Some constraints of this examination include that the considered numerical model is based on idealized conditions and may not accurately reflect real-world variability.

Future Research Directions:

The study opens several avenues for future research, particularly in exploring the effects of variable properties such as temperature-dependent viscosity and thermal conductivity, as well as more complex boundary conditions. Additionally, the use of the lattice Boltzmann method provides a valuable framework for extending these investigations to more realistic geometries and larger-scale systems, including those involving non-Newtonian fluids and multi-phase flow.

Conflicts of Interest

The authors declare no conflict of interest.

Data Availability

All data generated or analysed during this study are included in this article.

Notation

Roman

B	*Magnetic field intensity [Tesla]*
$c = \delta x/\delta t$	*streaming speed for LBM code.*
$C_S = c/\sqrt{3}$	*speed of the sound in the fluid flow field for LBM code*
e_i	*velocity in the D2Q9 lattice for the discrete type*
g	*Acceleration due to gravity [m/s²]*
L	*Width and height of square enclosure [m]*
Nu	*Nusselt number [-]*
p	*Dimensional pressure [Pa]*
T	*Dimensional temperature [K]*
$\bar{t}$	*Time (s)*
$\bar{u}, \bar{v},$	*Dimensional velocity components in* $\bar{x}, \bar{y} - coordinates$ *[m/s]*
w_i	*weighting coefficients.*
$\bar{x}, \bar{y},$	*Dimensional coordinates [m]*

Greek

α	*Thermal diffusivity [m²/s]*
β	*Thermal expansion coefficient [K⁻¹]*
μ	*Dynamic viscosity [kg/(ms)]*
ν	*Kinematic viscosity [m²/s]*
ρ	*Density of base fluid (water) [kg/m³]*
λ	Magnetic field inclination angle

Key parameter

Pr	Prandtl number ($\mathrm{Pr} = \upsilon/\alpha$)
Da	Darcy number ($Da = K/H^2$)
Gr	Grashof number ($Gr = g\beta(T_h - T_c)H^3/\upsilon$)
Ha	Hartmann number ($Ha = LB_0\sqrt{\sigma/\mu}$)
J	Joule magnetic parameter ($J = g\beta LHa^2/(c_p Ra)$)
Ri	Richardson number ($Ri = Gr/Re^2$)

ORCID

C. Venkata Lakshmi, https://orcid.org/0000-0003-2921-8129; **Anuradha Aravapalli,** https://orcid.org/0009-0003-5137-8804
K. Venkatadri, https://orcid.org/0000-0001-9248-6180; **O. Anwar Bég,** https://orcid.org/0000-0003-0614-8711
V. Ramachandra Prasad; https://orcid.org/0000-0002-9168-3825

REFERENCES

[1] Y.U.U.B. Turabi, and S. Munir, "CFD simulations of MHD effects on mixed convectional flow in a lid-driven square cavity with square cylinder using Casson fluid,' Numerical Heat Transfer, Part B: Fundamentals, pp.1-16 (2024). https://doi.org/10.1080/10407790.2024.2365890

[2] H.F. Oztop, and I. Dagtekin, "Mixed convection in two-sided lid-driven differentially heated square cavity," International Journal of Heat and Mass Transfer, **47**(8-9), 761-1769 (2004). http://dx.doi.org/10.1016/j.ijheatmasstransfer.2003.10.016

[3] R. Parveen, A.K. Hussein, T.R. Mahapatra, M. Al-Thamir, A. Abidi, M.B.B. Hamida, R.Z. Homod, and F.L. Rashid, "MHD double diffusive mixed convection and heat generation / absorption in a lid-driven inclined wavy enclosure filled with a ferrofluid," Int. J. Thermofluids, **22**, 100698 (2024). https://doi.org/10.1016/j.ijft.2024.100698

[4] O. Zikanov, I. Belyaev, Y. Listratov, P. Frick, N. Razuvanov, and V. Sviridov, "Mixed convection in pipe and duct flows with strong magnetic fields," Appl. Mech. Rev. **73**(1), 010801 (2021). https://doi.org/10.1115/1.4049833
[5] N.R. Devi, M. Gnanasekaran, A. Satheesh, P.R. Kanna, J. Taler, D.S. Kumar, *et al*., "Double-diffusive mixed convection in an inclined square cavity filled with nanofluid: A numerical study with external magnetic field and heated square blockage effects," Case Studies in Thermal Engineering, 56, 104210 (2024). https://doi.org/10.1016/j.csite.2024.104210
[6] P. Mondal, T.R. Mahapatra, R. Parveen, and B.C. Saha, "Heat Generation/Absorption in MHD double diffusive mixed convection of different nanofluids in a Trapezoidal enclosure," J. Nanofluids, **13**(2), 339-349 (2024). https://doi.org/10.1166/jon.2024.2116
[7] R. Parveen, and T. R. Mahapatra, "Heat and mass source effect on MHD double diffusive mixed convection and entropy generation in a curved enclosure filled with nanofluid," Nonlin. Analy. Model. Control, **27**(2) 308-330 (2022). https://doi.org/10.15388/namc.2022.27.25338
[8] Q. Yu, H. Xu, and S. Liao, "Analysis of mixed convection flow in an inclined lid driven enclosure with Buongiorno's nanofluid model," Int. J. Heat Mass Transf. **126**, 221-236 (2018). https://doi.org/10.1016/j.ijheatmasstransfer.2018.05.109
[9] Z. Mahmood, and U. Khan, "Mixed convective flow of nanofluid across exponential surface: A numerical assessment of the impact of Darcy-Forchheimer and nanoparticle aggregation," Numerical Heat Transfer, Part A: Applications, **86**(7), 1-26 (2023). https://doi.org/10.1080/10407782.2023.2288265
[10] M.J.H. Munshi, M.A. Alim, A.H. Bhuiyan, and M. Ali, "Hydrodynamic mixed convection in a lid-driven square cavity including elliptic shape heated block with corner heater," Procedia engineering, **194**, 442-449 (2017). https://doi.org/10.1016/j.proeng.2017.08.169
[11] S. Sivasankaran, V. Sivakumar, and A.K. Hussein, "Numerical study on mixed convection in an inclined lid-driven cavity with discrete heating," International Communications in Heat and Mass Transfer, **46**, 112-125 (2013). https://doi.org/10.1016/j.icheatmasstransfer.2013.05.022
[12] K.M. Khanafer, and J. Chamkha, "Mixed convection flow in a lid-driven enclosure filled with a fluid-saturated porous medium," Int. J. Heat Mass Transf. **42**(13), 2465–2481 (1999). https://doi.org/10.1016/S0017-9310(98)00227-0
[13] M.J.H. Munshi, N. Jahan, and G. Mostafa, "Mixed Convection Heat Transfer of Nanofluid in a Lid-Driven Porous Medium Square Enclosure with Pairs of Heat Source Sinks," Am. J. Eng. Res. (AJER), **8**(6), 59-70 (2019).
[14] Y. Nawaz, M.S. Arif, K. Abodayeh, and A.H. Soori. "A two-stage multi-step numerical scheme for mixed convective Williamson nanofluid flow over flat and oscillatory sheets," International Journal of Modern Physics B, **38**(22), 2450298 (2024). https://doi.org/10.1142/S0217979224502989
[15] D. Qaiser, Z. Zheng, and M.R. Khan, "Numerical assessment of mixed convection flow of Walters-B nanofluid over a stretching surface with Newtonian heating and mass transfer," Thermal Sci. Eng. Prog. 22, 100801 (2021). https://doi.org/10.1016/j.tsep.2020.100801
[16] M.A. Sheremet, M.S. Astanina, and I. Pop, "MHD natural convection in a square porous cavity filled with a water-based magnetic fluid in the presence of geothermal viscosity," International Journal of Numerical Methods for Heat & Fluid Flow, **28**(9), 2111-2131 (2018). https://doi.org/10.1108/HFF-12-2017-0503
[17] M.S. Alam, M.S.H. Mollah, M.A. Alim, and M.K.H. Kabir, «Finite Element Analysis of MHD Natural Convection in a Rectangular Cavity and Partially Heated Wall," Engineering and Applied Sciences, **10**(4), 53-58 (2017). https://doi.org/10.11648/j.eas.20170203.12
[18] B.P. Geridonmez, and H.F. Oztop, "Mixed Convection Heat Transfer in a Lid-Driven Cavity under the Effect of a Partial Magnetic Field," Heat Transfer Engineering, **42**(10), 875–887 (2020). https://doi.org/10.1080/01457632.2020.1792622
[19] S.S. Suchana, and M.M. Ali, "Finite Element Analysis of Convective Heat Transfer in a Linearly Heated Porous Trapezoidal Cavity in the Presence of a Magnetic Field," Int. J. Appl. Comput. Math. **10**, 141 (2024). https://doi.org/10.1007/s40819-024-01770-0
[20] C.G. Mohan, and A. Satheesh, "The Numerical Simulation of Double-Diffusive Mixed Convection Flow in a Lid-Driven Porous Cavity with Magnetohydrodynamic Effect," Arab. J. Sci. Eng. **41**, 1867–1882 (2016). https://doi.org/10.1007/s13369-015-1998-x
[21] N.A. Bakar, R. Roslan, A. Karimipour, and I. Hashim, "Mixed convection in lid-driven cavity with inclined magnetic field," Sains Malaysiana, **48**(2), 451-471 (2019). http://dx.doi.org/10.17576/jsm-2019-4802-24
[22] H. Moria, "Natural convection in an L-shape cavity equipped with heating blocks and porous layers," International Communications in Heat and Mass Transfer, **126**, 105375 (2021). https://doi.org/10.1016/j.icheatmasstransfer.2021.105375
[23] Y. Wang, G. Qin, W. He, and Z. Bao, "Chebyshev spectral element method for natural convection in a porous cavity under local thermal non-equilibrium model," International Journal of Heat and Mass Transfer, **121**, 1055-1072 (2018). https://doi.org/10.1016/j.ijheatmasstransfer.2018.01.024
[24] A. Nee, "Hybrid Lattice Boltzmann Simulation of Three-Dimensional Natural Convection," Journal of Computational and Theoretical Transport, **50**(4), 280–296 (2021). https://doi.org/10.1080/23324309.2021.1942061
[25] S.A. Fanaee, A. Shahriari, and S. Nikpour, "The Lattice Boltzmann Simulation of Free Convection Heat Transfer of a Carbon-Nanotube Nanofluid in a Triangular Cavity with a Solar Heater," Journal of Nanofluids, **13**(3), 694-709 (2024). https://doi.org/10.1166/jon.2024.2159
[26] A. Mahmoudi, I. Mejri, M.A. Abbassi, and A. Omri, "Lattice Boltzmann simulation of MHD natural convection in a nanofluid-filled cavity with linear temperature distribution," Powder Technology, **256**, 257-271 (2014). https://doi.org/10.1016/j.powtec.2014.02.032
[27] G.R. Kefayati, "Lattice Boltzmann simulation of natural convection in a square cavity with a linearly heated wall using nanofluid," Arabian Journal for Science and Engineering, **39**(3), 2143-2156 (2014). https://doi.org/10.1007/s13369-013-0748-1
[28] R.K. Tiwari, and M.K. Das, "Heat transfer augmentation in a two-sided lid-driven differentially heated square cavity utilizing nanofluids." Int. J. Heat Mass. Transf. **50**, 2002–2018 (2007). https://doi.org/10.1016/j.ijheatmasstransfer.2006.09.034
[29] R. Iwatsu, J.M. Hyun, and K. Kuwahara, "Mixed convection in a driven cavity with a stable vertical temperature gradient," Int. J. Heat Mass Transf. **36**, 1601–1608 (1993). https://doi.org/10.1016/S0017-9310(05)80069-9
[30] M.K. Moallemi, and K.S. Jang, "Prandtl number effects on laminar mixed convection heat transfer in a lid-driven cavity," International Journal of Heat and Mass Transfer, **35**(8), 1881-1892 (1992). https://doi.org/10.1016/0017-9310(92)90191-T

ВПЛИВ ДЖОУЛЕВОГО НАГРІВАННЯ ТА ГІДРОМАГНІТНИХ ЕФЕКТІВ НА ЗМІШАНУ КОНВЕКЦІЮ В ПОРИСТІЙ ПОРОЖНИНІ З ВИКОРИСТАННЯМ МЕТОДУ БОЛЬЦМАНА З ГРАТКОЮ

С. Венката Лакшмі[a], Анурадха Аравапаллі[a], К. Венкатадрі[b], О. Анвар Бег[c], В. Рамачандра Прасад[d]

[a]Кафедра прикладної математики, Шрі Падмаваті Махіла Вішвавідьялаям, Тірупаті, Андхра-Прадеш - 517502, Індія

[b]Кафедра математики, Університет Мохана Бабу (колишній інженерний коледж Шрі Відьянікетан), Тірупаті, Андхра-Прадеш - 517 102, Індія

[c]Група багатофізичних інженерних наук, Аеронавтика/Машинобудування, Університет Солфорда, Лабораторія корозії, 3-08, будівля SEE, Манчестер, M54WT, Велика Британія

[d]Кафедра математики, Школа передових наук, Технологічний інститут Веллор, Веллор, Таміл Наду 632014, Індія

У цій статті проводиться комплексне дослідження теплопередачі під впливом кількох факторів, включаючи магнітне поле, рухому кришку, пористе середовище та джоулеве нагрівання в порожнині з кришкою (LDC). Порожнина має рухому кришку, вертикальні стінки з теплоізольованими межами та горизонтальні стінки, що підтримуються при рівномірних температурах Th (внизу) та Tc (вгорі). Метою дослідження є аналіз поведінки змішаної конвективної теплопередачі системи за допомогою контурних діаграм для візуалізації потоку та теплової картини за різних розглянутих параметрів: числа Річардсона ($0{,}01 \le Ri \le 10$) та параметри джоулеве нагрівання ($0 \le J \le 10^{-5}$), числа Гартмана ($0 \le Ha \le 30$) та числа Дарсі ($0{,}001 \le Da \le 0{,}1$). Для використання основних рівнянь переносу застосовується метод ґратчастого Больцмана (LBM). Ефекти джоулевої термічної обробки є критично важливими в системах, де необхідно контролювати внутрішнє теплоутворення, наприклад, в електричних системах або охолодженні акумуляторів, де резистивна термічна обробка може як сприяти, так і перешкоджати бажаній тепловій динаміці.

Ключові слова: *метод Больцмана з ґраткою (LBM); порожнина з кришкою; магнітогідродинаміка; змішана конвекція; джоулева термічна обробка; пористе середовище*